MATERIALS AND MANUFACTURING PROCESSES
2018, VOL. 33, NO. 14, 1587–1593
https://doi.org/10.1080/10426914.2018.1424905

Taylor & Francis
Taylor & Francis Group

Selective electrochemical machining of the steel molds in hot isostatic pressing of Ti6Al4V powder

Fabio Scherillo, Antonello Astarita, Umberto Prisco, and Antonino Squillace

Department of Chemical, Materials and Production Engineering, University of Napoli Federico II, Napoli, Italy

ABSTRACT

Anodic dissolution is proven to be an effective method to remove stainless steel molds from Ti6Al4V compacts obtained from powder by hot isostatic pressing. Two different working solutions were studied: 2 M NaCl and 2 M NaCl + 0.05 M Na_2EDTA. While both were capable of removing the steel mold, the latter was also capable of removing the diffusional layer made by the intermetallic phases generated between titanium and steel during the compaction process.

ARTICLE HISTORY
Received 21 June 2017
Accepted 22 December 2017

KEYWORDS
AISI 304; anodic; chlorides; dissolution; EDTA; intermetallics; sintering; Ti6Al4V

Introduction

Electrochemical machining is a fast and effective technology to manufacture products through removing metal from a workpiece by a controlled anodic dissolution in a neutral solutions (e.g., an aqueous solution of sodium nitrate) at extremely large current densities, up to 100 A/cm^2.[1,2] Among the important advantages of this technique, it is worth mentioning: it is a forceless machining, produces no thermal stress and no tool wear, the material removal rate is independent from the surface hardness, allows the generation of complex shapes without the need of further operations. As drawback, electrochemical machining is a multivariable process whose study and modeling requires detailed knowledge of corrosion, passivation, and interface reaction kinetics. Being the basic mechanism of electrochemical machining, anodic behavior is the key factor governing the machinability of a material.[3] Numerous studies have focused on the anodic mechanism in different materials, including Fe,[4–6] Al,[7] Cu,[8,9] Ni,[10] Co,[11,12] and their alloys.[13,14] However, very little work has been conducted on titanium and its alloys.[15–17] To the authors' best knowledge, there are still no paper dealing with the study of the anodic dissolution in the presence of interfaces between dissimilar materials and with complex and nonuniform microstructure. This can be the case of the removal of steel mold from a hot isostatic pressed titanium compact.

Hot isostatic pressing (HIP) is an interesting process to produce highly compacted components with a very low residual porosity. This is of particular value in powder metallurgy, where the presence of microporosity is an acknowledged drawback. During the process, a sheet metal mold, usually made of stainless steel, is filled with powder and then compacted at high pressure and temperature in a furnace. The compaction is achieved by the contemporary application of pressure and high temperature so that two different mechanisms of mass transport can be activated: diffusion and plastic flow.[18,19] It is clear that the mold needs to be removed at the last step of the process.

In the production of HIPed titanium component, the pressure can reach up to 1300 bar, while the temperature can range between 1073 and 1373 K. At temperatures and pressures so high, a strong diffusion bonding, characterized by the formation of different intermetallics, occurs between the titanium powder and steel mold.[20,21] As described in a previous paper of the authors,[22] the result is the formation of a titanium–steel interface interposed between the titanium compact and steel mold. Having different microstructure and properties with respect to the bulk material of the mold and of the compact, this interface must be removed before the HIPed component could be set working.

In general, the HIP molds are removed through conventional machining, but there are two main problems linked to this approach: (i) complex-shaped molds are difficult or even impossible to remove; (ii) the removal of the interface layer is difficult to control, considering that its thickness is not known *a priori*.

From this point of view, the anodic dissolution can be a process full of promises in regard to the removal of steel mold and interface layer. This is based on the ability to tailor the variables of the process so that only the steel mold and Fe compounds can be removed without damaging the Ti6Al4V part. So far, the dissolution of stainless steel molds has been studied and discussed in previously cited literature, but never in relation with the use of titanium powder. In this paper, the conditions needed for the complete removal of steel mold and the interface diffusion zone are studied. In particular, the different electrochemical behavior of steel and Ti6Al4V is

CONTACT Antonello Astarita antonello.astarita@unina.it Department of Chemical, Materials and Production Engineering, University of Napoli Federico II, Piazzale Tecchio 80, 80125 Napoli, Italy.
Color versions of one or more figures in the article can be found online at www.tandfonline.com/lmmp.

exploited to selectively dissolve the steel and the titanium–steel interface without damaging the bulk-sintered compact.

Concentrated saline solutions have been proved to be effective in anodic dissolution of steel,[23,24] while it is well known that titanium and its alloys have a high resistance to dissolution under these conditions. The question is then to find a way to dissolve the titanium–steel interface which develops during the HIP process. The ethylenediaminetetraacetic acid (EDTA), an aminopolycarboxylic acid, that forms very stable chelates in aqueous solution with the main constituent of stainless steel, Fe, Cr, and Ni, could resolve this problem. As will be discussed in details, the addition of EDTA to the electrochemical solution allows dissolving both the steel mold and the interface layer. The dissolution process therefore reaches the bulk of the compact demonstrating the possibility to produce a true near-net shape component.

Materials and Methods

The compact-mold system subject of this study was prepared using a Ti6Al4V powder with an average diameter of about 100 μm. The powder composition by weight percent is Al 6.1, V 4.2, Fe 0.07, Cu 0.05, Ti rest. The Ti6Al4V powder was poured into an AISI 304 cylindrical stainless steel mold 150 mm in length with 70 mm inner diameter and a thickness equal to 1.5 mm. The steel weight percent composition is 0.08 C, 18.5 Cr, 9.0 Ni, 2.0 Mn, 0.08 Si, 0.01 P, 0.01 S, Fe rest. The powder was compressed into the mold with a 500 bar hydraulic press assisted by vibrations to obtain a high initial packing density. The relative density of the cold-pressed compact ranged within 0.53–0.56. The packed molds were vacuum-heated to a temperature of 200°C and a void of 10^{-3} bar for 24 h to remove gas and moisture, then sealed by thermal welding. The sample was placed inside the hot isostatic press and heated up to the process temperature of 1100°C under an argon atmosphere. The pressure was increased in proportion to temperature up to the final level of 1300 bar. The heating and dwell stage of the process lasted 1.5 h, followed by cooling inside the furnace. At the end of the HIP process, the relative density reached close to 100%.

The experimental work about the dissolution of HIPed molds was split into three steps according to the sequence of layers engaged by the electrochemical machining from the outside to the compact bulk. The first step was the study of the optimal condition for the anodic dissolution of AISI 304 steel, the second one was the study of the optimal condition for the dissolution of titanium–steel interface, the last one was the verification of the passivation of the sintered titanium compact in regard to the optimal conditions found in the first two steps.

The electrochemical tests of the experimental activity were performed at room temperature in 2 M NaCl and in 2 M NaCl + 0.05 M Na_2EDTA aqueous solutions to show the importance of EDTA and compare the obtained results. All solutions were prepared using analytical-grade reagents. Potentiodynamic polarization measurements were performed in both the solutions at a scan rate of 0.2 mV/s in a conventional three-electrode cell using a graphite bar as a counterelectrode. The dissolution tests were run in galvanostatic mode with stagnant conditions and a current density of 0.5 A/cm^2 using the abovementioned solutions. A research-grade galvanostat/potentiostat (current range: 10 μA to 800 mA, current resolution: 760 pA, control voltage: ±10 V, voltage resolution: 5 μV, electrochemical impedance spectroscopy (EIS) measurement from 10 μHz to 1 MHz, acquisition time: 20 μs) was used. External boosters from 2 A up to 10 A were used during the electrochemical tests. Potentials were measured against a 3 M KCl Ag/AgCl reference electrode (+210 mV versus standard hydrogen electrode).

The assessment of potentiodynamic behavior of the 1.5-mm-thick AISI 304 steel, first objective of the experimental work, was studied by cold mounting 15 × 15 mm specimens of the sheet into epoxy resin, see Fig. 1(a) for the experimental setup and the arrangement of electrodes. Dissolution tests of the steel were made in galvanostatic mode and stagnant conditions with a current density of 0.5 A/cm^2 to determine the kinetics and mechanism of the electrode reactions. Furthermore, to better understand the mechanism of mold dissolution and the role played by the EDTA, the electrochemically machined surface of the specimen was analyzed by

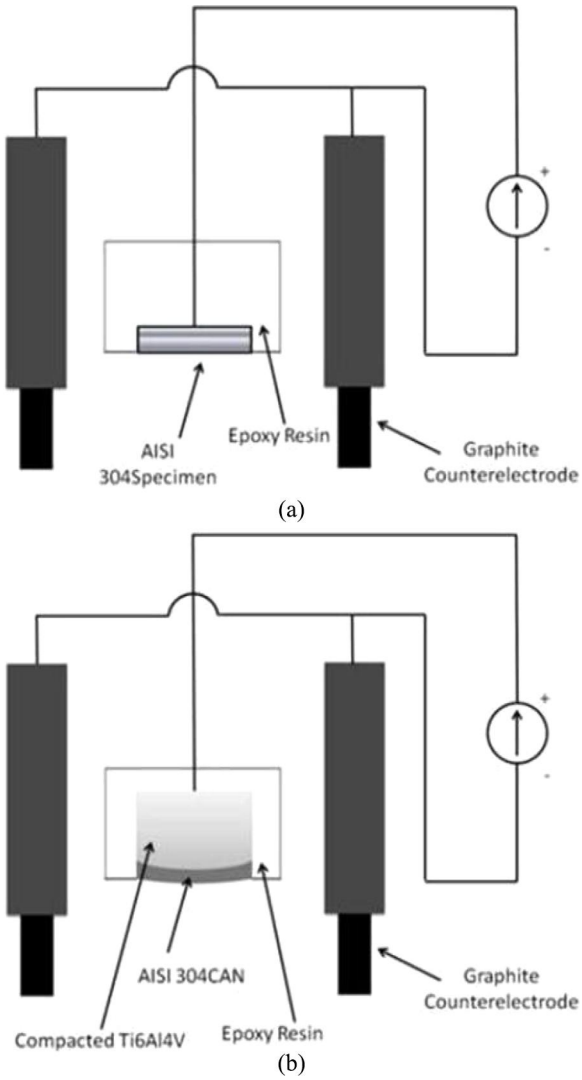

Figure 1. Experimental setup used in dissolution tests of (a) AISI 304 and (b) slice extracted from the HIPed workpiece.

scanning electron microscopy (SEM) and the composition measured through energy-dispersive X-ray microanalysis (EDXMA) operating at 15 keV. The EDX analysis was performed in scanning mode.

To fulfill the successive aims of the experimental study, namely, the dissolution of titanium–steel interface and the passivation of the compact, several specimens were extracted from the HIPed workpiece.

Some specimens were cut in the shape of slices presenting the external cylindrical surface of the mold, on one side, whereas the opposite surface points toward the compact core; the base face of these slices is depicted in Fig. 1(b). These specimens measure approximately 15 mm along the mold axis and 15 mm along the curved line of the cylindrical surface; the depth of the specimens was around 10 mm, enough to cover both the mold thickness and the interface zone while leaving enough of the bulk workpiece. The resultant specimens were cold mounted into epoxy resin for electrochemical machining, according to the setup of Fig. 1(b); obviously, the specimens are encapsulated with the steel mold surface left accessible. They were electrochemically machined in galvanostatic mode and stagnant condition at 0.5 A/cm^2 until the compete dissolution of both the mold and titanium–steel interface. The obtained surface was then analyzed by SEM and EDXMA.

Some other specimens were extracted from the bulk of HIPed Ti6Al4V material to study the mechanism of its passivation. Potentiodynamic polarizations tests were performed on these specimens under the same conditions used for the AISI 304 steel.

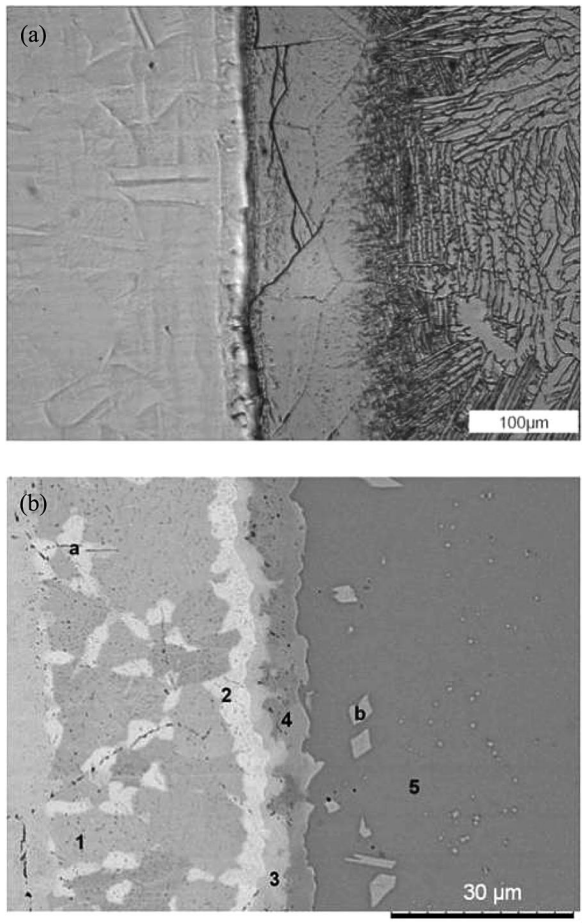

Figure 2. (a) Optical micrograph of the interface, (b) SEM micrograph of the interface with the indication of different zones.[25] AISI 304 mold (on the left) and the HIPed material (on the right).

Results and Discussion

Before analyzing the results of the electrochemical experiments, a description of the titanium–steel interface generated during the HIP process is necessary. More details about this interface can be found in a previous paper of the authors.[25] Figure 2(a) reports the SEM micrograph of the observed morphology from mold bulk to compact bulk. The interface extends for about 150 µm between the AISI 304 mold and HIPed material. Five different intermetallic zones can be distinguished in the close-up of Fig. 2(b). The composition and identification of these intermetallic phases are given in Table 1. Being their compositions and mechanical properties starkly different from that of the bulk compact, they need to be removed along with the steel mold. As discussed in the aforementioned paper, no signatures of hydrogen embrittlement were observed in the Ti6Al4V workpieces.

In Fig. 3, the results of potentiodynamic tests are reported. The qualitative features of potentiodynamic scanning in both the solutions for AISI 304 can be used to identify the following responses. A classical cathodic regime, in which the current is determined by the reduction of dissolved oxygen, is visible below −0.2 V. With an increase in potential, starting from −0.15 V, the regime become one in which metal oxidation is the dominant reaction taking place in the active region. The current in this regime rises as a function of the applied potential. A strong transpassive regime starts above the breakaway potential, 0.3 V for the 2 M NaCl solution, 0.4 V for the 2 M NaCl + 0.05 M Na_2EDTA solution. For potential higher than 0.7 V, the AISI 304 steel shows an anodic limiting current. On the contrary, the HIPed Ti6Al4V reaches a passive region above 0 V in both solutions. This implies that the mold can be selectively dissolved in both the solutions for potentials greater than 0.3 V, since the electrochemical machining will stop at the surface of the HIPed Ti6Al4V which is protected above this potential.

These findings are used as an input to the electrochemical machining tests. The dissolution of AISI 304 steel under galvanostatic condition proceeds in two stages, as shown by the results of galvanostatic dissolution at 0.5 A/cm^2 in Fig. 4. A first stage of lower duration at higher potential is followed by a second longer stage at lower potential. The first step lasts the time necessary for chlorides to induce the breakdown of the outer oxide layer protecting the AISI 304 specimen surface. As soon as the chlorides have induced the breakdown of the oxide, the bare metal is exposed to the solution and the dissolution process can begin. This behavior does not change between the two solutions throughout the dissolution. Indeed, the applied current density of 0.5 A/cm^2 is close to the value of the anodic limiting current, equal for both the solutions, as shown in the polarization curves. Under these conditions, the mechanics limiting the removal rate of the process is the mass transport from the surface of the metal to the bulk of the solution.

Table 1. Average wt% composition of the different zones of the titanium–steel interface built up during the HIP process. For Zone 5, maximum and minimum concentrations are given.[25]

Zone	Fe	Cr	Ni	Ti	Al	Phase
1	64.73	26.74	5.17	3.36		σ
2	63.23	23.18	5.00	8.59		χ
3	46.23	13.66	4.39	34.80	0.92	λ + FeTi
4	31.03	3.99	7.02	56.27	1.69	Ti_2Ni + (Fe,Ni)Ti + β-Ti
5	16.34–5.03	3.64–1.28	2.19–1.71	72.41–84.44	5.42–7.54	β-Ti + FeTi
a	60.19	24.21	6.61	8.99		χ
b	24.87	2.46	9.98	61.08	1.61	Ti_2Ni + (Fe,Ni)Ti + β-Ti

The dissolution reactions of AISI 304 stainless steel in concentrated chloride solution are summarized in Fig. 5, in which, for reason of simplicity, only reaction mechanisms involving Cr, which is the main constituent of the passive layer, are shown. Further details about the involved chemical reactions can be found in Milosev [26] and Mount et al.[27] According to the reaction path 1, the products of dissolution are Cr(VI), Fe(III), and Ni(II), whereas along the reaction path number 2, they are Cr(III), Fe(II), and Ni(II).

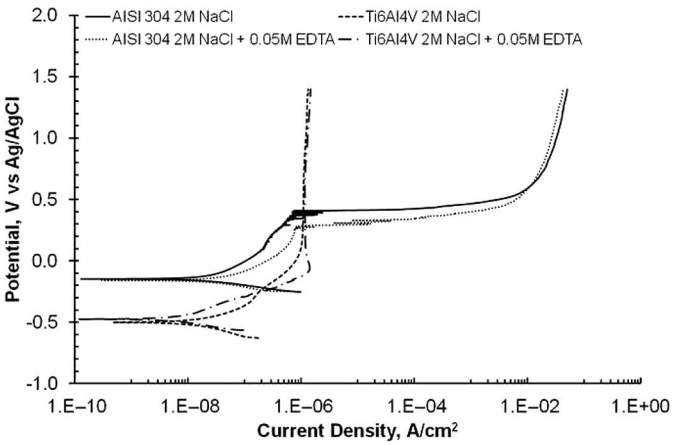

Figure 3. Potentiodynamic polarization curves of AISI 304 and HIPed Ti6Al4V in 2 M NaCl and 2 M NaCl + 0.05 M Na_2EDTA solutions.

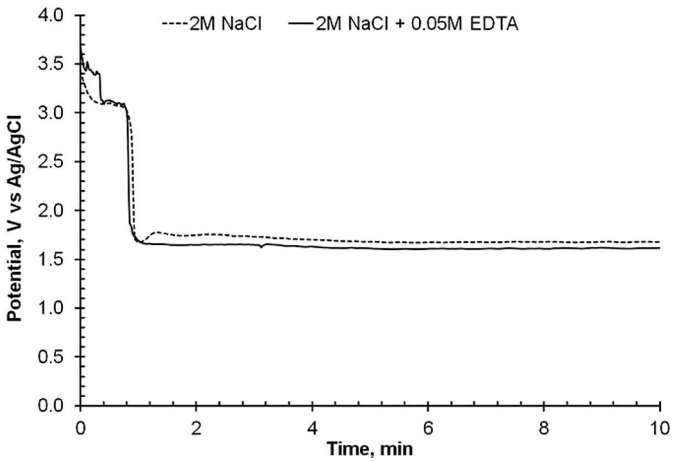

Figure 4. Galvanostatic potential–time curve for AISI 304.

These paths are intrinsically antithetic. As demonstrated by Bojinov et al.,[28] the transpassive dissolution of stainless steel through the formation of highly valent ions is a complex phenomenon that involves the peculiar structure of the passive layer with the contribution of different phenomena in competition with each other. For example, chloride ions can induce strong modifications in that structure that inhibits mechanism 1.[29,30] The dissolution occurs through the breakdown of the passive film along the reaction paths 1 and 2, while the reaction path 3 is in competition with the oxidation mechanisms.

To find out the prevalent dissolution path under the chosen experimental conditions, the apparent valence of dissolution, *n*, was determined from the weight loss measured in galvanostatic mode using Faraday's law in the hypothesis of efficiency equal to 100%[27]:

$$n = \frac{i \cdot A \cdot t}{\Delta m \cdot F} \mathrm{MW} \tag{1}$$

In Equation (1), *i* is the current density, *A* the exposed area of the specimen, Δm the weight loss at the time *t*, *F* Faraday's constant (96485.3 C/mol), and MW the average molecular weight of the alloy. The calculate valences are $n = 2.25$ for the 2 M NaCl solution and $n = 2.24$ for the 2 M NaCl + 0.05 M Na_2EDTA solution. By comparison of the experimental results with the theoretical values, $n = 3.48$ for mechanism 1 and $n = 2.19$ for mechanisms 2 and 3, it is possible to deduce that in this case the dissolution of AISI 304 does not occur through the formation of highly valent ions.

Further details about the role of EDTA are deduced by the SEM and EDXMA analyses performed on the surface of the AISI 304 specimen after the galvanostatic test. Results of

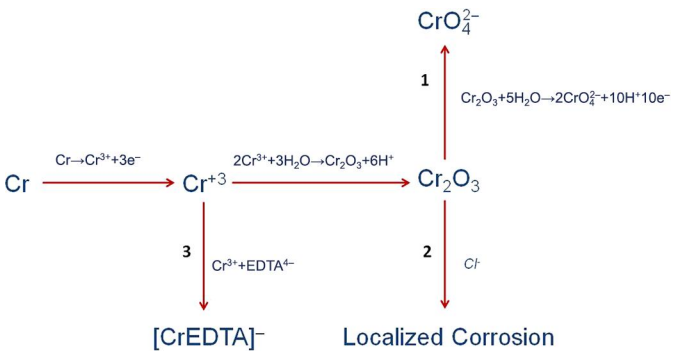

Figure 5. Simplified network of the reactions occurring during the anodic dissolution of AISI 304 steel.

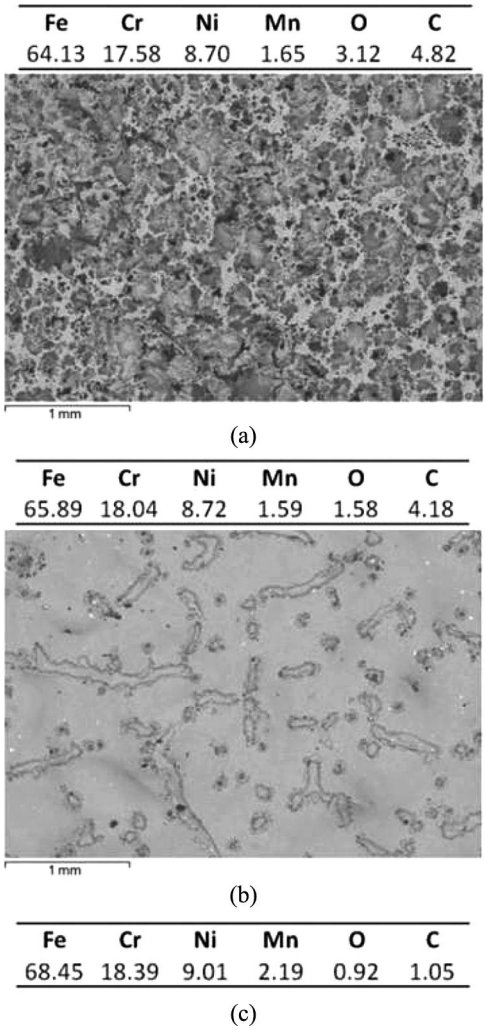

Figure 6. (a) Morphology and measured wt% composition of the AISI 304 surface after galvanostatic test in 2 M NaCl solution, (b) morphology and measured wt% composition of the AISI 304 surface after galvanostatic test in 2 M NaCl + 0.05 M EDTA solution, (c) measured wt% composition of the as-received AISI 304 surface.

the analyses for the two solutions are reported in Fig. 6, along with the measured composition of the base material. Due to its accuracy limitations, EDX can be used only to estimate the weight ratio of the components of an alloy. In this study, EDX is used in semiquantitative manner to determine if the treatment had caused changes in the weight ratio of an element compared to the base material. Taking into account the sensitivity that can be usually achieved on modern spectrometers, a difference of more than 2% on the detected value of the wt% is considered statistically significant.

The morphology of the steel surface after dissolution in 2 M NaCl shows a typical localized corrosion with a carbon- and oxygen-enriched composition with respect to the surface of the base material. On the contrary, the morphology of the steel surface after dissolution in 2 M NaCl + 0.05 M Na_2EDTA presents both areas of localized corrosion and areas which underwent uniform dissolution. Furthermore, a lower concentration of oxygen is detected in the surface treated by galvanostatic test in 2 M NaCl + 0.05 M Na_2EDTA. This is in agreement with the results obtained by Kocijan et al.[31] about the effect of complexing agent on the corrosion of stainless steels for biomedical applications. In this study, the authors observed that one of the effects of EDTA and other chelating molecules is the reduction of the oxygen contents in the metal surface exposed to an environment capable of inducing localized corrosion.

As expected, the dissolution of HIPed specimen, reported in Fig. 7, proceeds in two stages as well as for the AISI 304. In the second stage, the galvanostatic potential–time curve slowly increases due to the curvature of the metal surface exposed to the solution. Indeed, the cylindrical shape of the mold brings about a decrease in the exposed area as the dissolution progresses so that the current density, and consequently the potential, needs to increase under the constraint of constant current intensity. The final part of the curve is characterized by a sharp increase in the potential with the passing of the time. This zone corresponds to the beginning of the oxygen evolution on the metal surface and to the end of dissolution process.

Scanning electron microscopy and EDXMA analyses on the worked surface are shown in Fig. 8. In the case of 2 M NaCl, the composition of the surface indicates that the electrochemical machining stopped approximately between zones 2 and 3 of the titanium–steel interface layers reported in Table 1. On the contrary, the composition of the surface after dissolution in 2 M NaCl + 0.05 M EDTA matches the composition of the very end of the zone 5, as determined by the previous analyses, see Fig. 2 and Table 1. This indicates that the whole titanium–steel interface formed during the HIP process was removed and the dissolution reached the bulk of the TI6Al4V compact. The lamellar morphology visible in the optical micrograph in Fig. 8(b), very similar to the bulk microstructure of the Ti6Al4V HIPed compact, confirms this conclusion. In Figs. 9 and 10, interface images showing the removal, respectively, without EDTA and with EDTA, are reported. It is possible to appreciate that the EDTA allows the removal of intermetallic layer that remains untouched when the EDTA is not used in the solution.

The presence of EDTA determines the different development of the electrochemical machining in the two analyzed solutions. In the case of 2 M NaCl as the dissolution

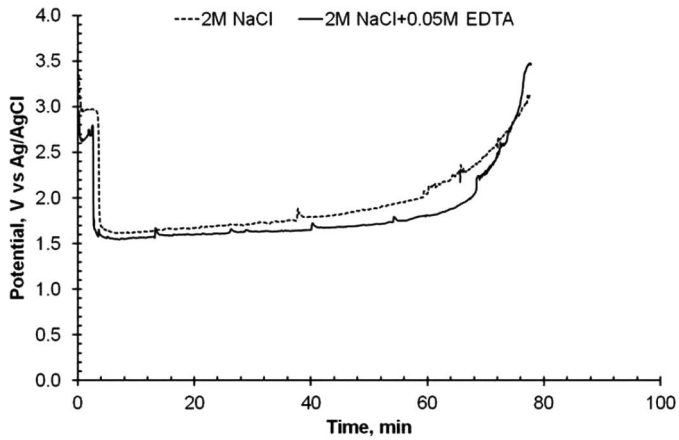

Figure 7. Galvanostatic potential–time curve for the dissolution of HIPed workpiece in 2 M NaCl and 2 M NaCl + 0.05 M Na_2EDTA solutions.

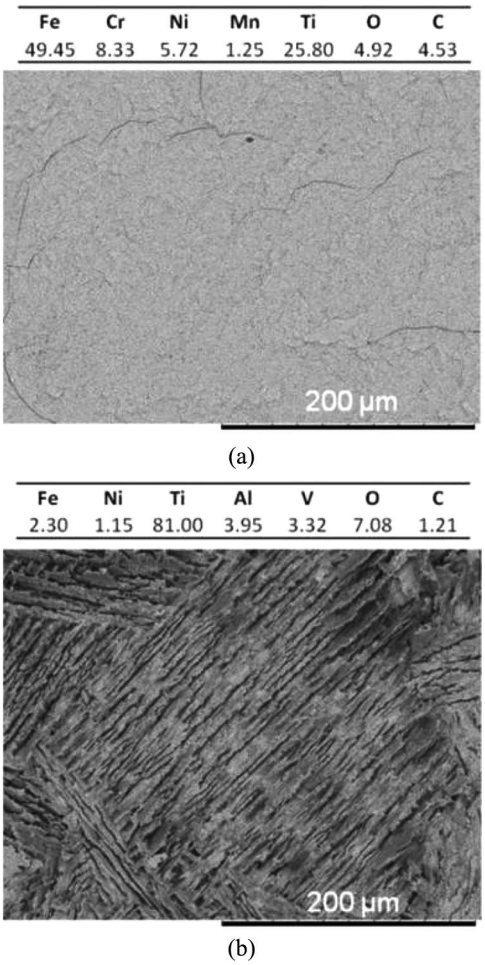

Figure 8. (a) Morphology and measured wt% composition of surface obtained after dissolution of the mold in 2 M NaCl solution, (b) morphology and measured wt% composition of surface obtained after dissolution of the mold in 2 M NaCl + 0.05 M Na_2EDTA solution.

progresses, the solution reaches zones of higher and higher Ti content, so that the reactions reported in Fig. 11 are progressively triggered. In particular, the chlorides promote, through

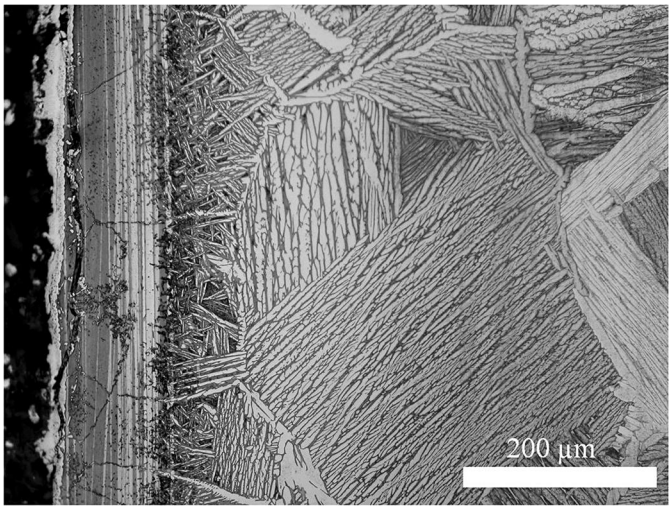

Figure 9. Interface SEM image showing the removal in 2 M NaCl solution. *Note*: SEM, scanning electron microscopy.

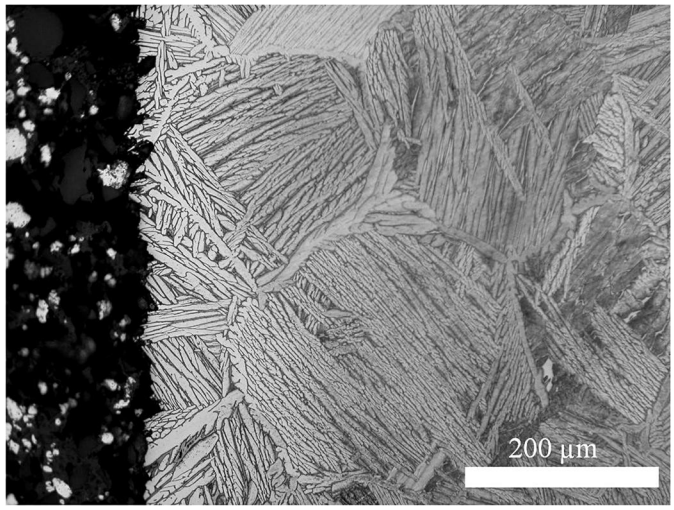

Figure 10. Interface SEM image showing the removal in 2 M NaCl + 0.05 M Na_2EDTA solution. *Note*: SEM, scanning electron microscopy.

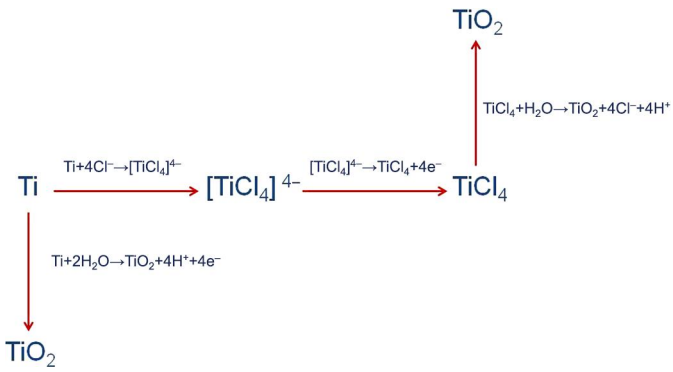

Figure 11. Chemical reactions for the formation of protective TiO_2 induced by the presence of chlorides.

the chemisorbed complex $[TiCl_4]^{4-}$, the formation of titanium dioxide which being highly protective acts as an effective barrier against the dissolution and stops at the very beginning the machining of the tintanium–steel interface. Conversely, the EDTA promotes the solubilization of Fe, Cr, and Ni through the formation of highly stable complex ions, as $[CrEDTA]^{-}$, $[FeEDTA]^{2-}$, and $[NiEDTA]^{2-}$. The consequence is that the dissolution does not stop at the interface but proceeds until the reach of the bulk of the Ti6Al4V compact. Furthermore, in the presence of EDTA, it is also possible that a selective dealloying occurs in the Ti-rich zones of the interface leading to the production of a weak structure which helps the dissolution process.

Conclusion

Anodic dissolution allows the removal of AISI 304 steel mold from Ti6Al4V HIPed compacts; the dissolution proceeds exploiting the transpassive behavior of the steel with localized corrosion in 2 M NaCl solution. The dissolution is also helped in the presence of EDTA by the formation of chelates.

The 2 M NaCl solution is capable of removing the steel mold but not the titanium–steel interface formed during the HIP process. On the contrary, the addition of EDTA enables the dissolution of both the mold and interface until the machining reaches the bulk of the Ti6Al4V compact.

As soon as the surface of the bulk of the compact is reached, the process stops because of the passivation of Ti6Al4V taking place under the chosen processing conditions.

Under the proposed conditions, the electrochemical machining acts as a highly selective process since it dissolves the mold and titanium–steel interface but stops at the bulk compact. The usefulness of this result in the field of industrial applications cannot be overstated.

Acknowledgment

The authors thank Dr Antonella Scherillo (STFC Rutherford Appleton Laboratory) for helpful comments and discussion on the manuscript. Dr Claudio Testani (CSM) is acknowledged for his guidance and support. The authors acknowledge Antonio Castiello for his assistance with the experimental work.

Funding

This work was funded by the Italian Ministry for Education, University and Research (grant PON01_00538, TITAFORM).

References

[1] Wilson, J. F. *Practice and Theory of Electrochemical Machining*, 2nd ed.; John Wiley & Sons Inc., 1971; pp 87.
[2] Lohrengel, M. M.; Rataj, K. P.; Münninghoff, T. Electrochemical Machining—Mechanisms of Anodic Dissolution. *Electrochim. Acta* **2016**, *201*, 348–353.
[3] Liu, W.; Ao, S.; Li, Y.; Liu, Z.; Zhang, H.; Manladan, S. M.; Wang, Z. Effect of Anodic Behavior on Electrochemical Machining of TB6 Titanium Alloy. *Electrochim. Acta* **2017**, *233*, 190–200.
[4] Judal, K. B.; Yadava, Y. Experimental Investigations into Electrochemical Magnetic Abrasive Machining of Cylindrical Shaped Nonmagnetic Stainless Steel Workpiece. *Mater. Manuf. Process.* **2013**, *28*(10), 1095–1101.
[5] Guo, K.; Li, M.; Gong, Q.; Li, C.; Li, C.; Zhong, H.; Zhou, Y. Experimental Investigation on Steel Foams Fabricated by Sintering-Dissolution Process. *Mater. Manuf. Process.* **2016**, *21*(12), 1–6.
[6] Saraf, A. R.; Sadaiah, M. Magnetic Field-Assisted Photochemical Machining (MFAPCM) of SS316 L. *Mater. Manuf. Process.* **2017**, *32*(3), 327–332.
[7] Sankar, M.; Gnanavelbabu, A.; Rajkumar, K.; Thushal, N. A. Electrolytic Concentration Effect on the Abrasive Assisted-Electrochemical Machining of an Aluminum–Boron Carbide Composite. *Mater. Manuf. Process.* **2017**, *32*(6), 687–692.
[8] Li, W.; Guo, D.; Jin, Z.; Wang, Z.; Yuan, Z. Electrochemical Mechanical Polishing of Copper with High Permittivity Abrasives. *Mater. Manuf. Process.* **2013**, *28*(2), 207–212.
[9] Schneider, M.; Schroth, S.; Richter, S.; Hohn, S.; Schubert, N.; Michaelis, A. In-situ Investigation of the Interplay between Microstructure and Anodic Copper Dissolution Under Near-ECM Conditions - Part 2: The Transpassive State. *Electrochim. Acta* **2012**, *70*, 76.
[10] Huang, S. F.; Liu, Y. Electrochemical Micromachining of Complex Shapes on Nickel and Nickel-Based Superalloys. *Mater. Manuf. Process.* **2014**, *29*(11–12), 1483–1487.
[11] Schneider, M.; Schroth, S.; Richter, S.; Hohn, S.; Michaelis, A. Anodic Dissolution Behaviour and Surface Texture Development of Cobalt Under Electrochemical Machining Conditions. *Electrochim. Acta* **2013**, *106*, 279.
[12] Schubert, N.; Schneider, M.; Michaelis, A. The Mechanism of Anodic Dissolution of Cobalt in Neutral and Alkaline Electrolyte at High Current Density. *Electrochim. Acta* **2013**, *113*, 748.
[13] Shaikh, J. H.; Jain, N. K.; Venkatesh, V. C. Precision Finishing of Bevel Gears by Electrochemical Honing. *Mater. Manuf. Process.* **2013**, *28*(10), 1117–1123.
[14] Zhao, Z.; Gao, J.; Wei, L.; Chui, K. Tungsten Wires and Porous NiAl Prepared through Directional Solidification and Selective Dissolution. *Mater. Manuf. Process.* **2017**, *32*, 1817–1822.
[15] Bannard, J. On the Electrochemical Machining of Some Titanium Alloys in Bromide Electrolytes. *J. Appl. Electrochem.* **1975**, *6*, 477.
[16] Gonzalez, J.E. G.; Mirza-Rosca, J. C. Study of the Corrosion of Titanium and Some of Its Alloys for Biomedical and Dental Implant Applications. *J. Electroanal. Chem.* **1999**, *471*, 109.
[17] Pan, J.; Thierry, D.; Leygraf, C. Electrochemical Impedance Spectroscopy Study of the Passive Oxide Film on Titanium for Implant Application. *Electrochim. Acta* **1996**, *41*, 1143.
[18] Kim, K. T.; Yang, H. C. Densification Behavior of Titanium Alloy Powder Under Hot Isostatic Pressing. *Powder Metall.* **2001**, *44*(1), 41–47. DOI: 10.1179/003258901666158.
[19] Atkinson, H. V.; Davies, S. Fundamental Aspects of Hot Isostatic Pressing: An Overview. *Metall. Mater. Trans. A* **2000**, *31*(12), 2981–3000.
[20] Swarup, K. G.; Chatterjee, S. On the Direct Diffusion Bonding of Titanium Alloy to Stainless Steel. *Mater. Manuf. Process.* **2010**, *25*(11), 1317–1323. DOI: 10.1080/10426914.2010.520793.
[21] Aleman, B.; Gutierrez, I.; Urcola, J. J. Interface Microstructures in Diffusion Bonding of Titanium Alloys to Stainless and Low Alloy Steels. *Mater. Sci. Technol.* **1993**, *9*(8), 633–641. DOI: 10.1179/mst.1993.9.8.633.
[22] Scherillo, F.; Aprea, P.; Astarita, A.; Scherillo, A.; Testani, C. Squillace, A. On the Interface Generated by Hot Isostatic Pressing Compaction Process Between an AISI 304 Container and the Ti6Al4V Powders. *Metall. Mater. Trans. A* **2015**, *46*(6), 2376–2379. DOI: 10.1007/s11661-015-2868-6.
[23] Tang, L.; Guo, Y.-F. Experimental Study of Special Purpose Stainless Steel on Electrochemical Machining of Electrolyte Composition. *Mater. Manuf. Process.* **2013**, *28*(4), 457–462. DOI: 10.1080/10426914.2012.746784.
[24] Thanigaivelan, R.; Arunachalam, R. M. Experimental Study on the Influence of Tool Electrode Tip Shape on Electrochemical Micromachining of 304 Stainless Steel. *Mater. Manuf. Process.* **2010**, *25*(10), 1181–1185. DOI: 10.1080/10426914.2010.508806.
[25] Scherillo, F.; Aprea, P.; Astarita, A.; Scherillo, A.; Testani, C.; Squillace, A. On the Interface Generated by Hot Isostatic Pressing Compaction Process Between an AISI 304 Container and the Ti6Al4V Powders. *Metall. Mater. Trans. A* **2015**, *46*(6), 2376–2379. DOI: 10.1007/s11661-015-2868-6.
[26] Milosev, I. Effect of Complexing Agents on the Electrochemical Behaviour of Orthopaedic Stainless Steel in Physiological Solution. *J. Appl. Electrochem.* **2002**, *32*(3), 311–320.
[27] Mount, A. R.; Howarth P. S.; Clifton, D. The Electrochemical Machining Characteristics of Stainless Steels. *J. Electrochem. Soc.* **2003**, *150*(3), D63–D69. DOI: 10.1149/1.1545463.
[28] Bojinov, M.; Betova, I.; Fabricius, G.; Laitinen, T.; Raicheff, R.; Saario, T. The Stability of the Passive State of Iron–Chromium Alloys in Sulphuric Acid Solution. *Corrosion Sci.* **1999**, *41*(8), 1557–1584. DOI: 10.1016/S0010-938X(99)00003-7.
[29] Schultze, J. W.; Lohrengel, M. M. Stability, Reactivity and Breakdown of Passive Films. Problems of Recent and Future Research. *Electrochim. Acta* **2000**, *45*(15–16), 2499–2513. DOI: 10.1016/S0013-4686(00)00347-9.
[30] Olsson, C.-O.A.; Landolt, D. Passive Films on Stainless Steels-Chemistry, Structure and Growth. *Electrochim. Acta* **2003**, *48*(9), 1093–1104. DOI: 10.1016/S0013-4686(02)00841-1.
[31] Kocijan, A.; Milosev, I.; Pihlar, B. The Influence of Complexing Agent and Proteins on the Corrosion of Stainless Steels and Their Metal Components. *J. Mater. Sci. Mater. Med.* **2003**, *14*(1), 69–77. DOI: 10.1023/A:1021505621388.